LWT - Food Science and Technology 231 (2025) 118299

Contents lists available at ScienceDirect

LWT

journal homepage: www.elsevier.com/locate/lwt

Mineral profile, oxidative stability and color traits in dry aged Meat: Integrative analysis

Ana J. Ribeiro [a,b,*], Fernando G. Braga [c,d], Irene Oliveira [e,f], Filipe Silva [a,b], Paula Teixeira [g], Cristina M. Saraiva [a,b]

[a] CECAV—Centre for Studies in Animal and Veterinary Science, University of Trás-Os-Montes and Alto Douro (UTAD), Vila Real, Portugal
[b] AL4AnimalS—Associate Laboratory for Animal and Veterinary Sciences, Vila Real, Portugal
[c] Department of Chemistry, University of Trás-os-Montes e Alto Douro (UTAD), Vila Real, Portugal
[d] Chemistry Research Centre - Vila Real (CQ-VR), University of Trás-os-Montes e Alto Douro (UTAD), Vila Real, Portugal
[e] Department of Mathematics, School of Science and Technology, UTAD, 5000-801, Vila Real, Portugal
[f] Center for Computational and Stochastic Mathematics (CEMAT), IST-UL, Portugal
[g] Universidade Católica Portuguesa, CBQF - Centro de Biotecnologia e Química Fina– Laboratório Associado, Escola Superior de Biotecnologia, Rua de Diogo Botelho 1327, 4169- 005, Porto, Portugal

ARTICLE INFO

Keywords:
Dry aged beef
Aging process
Lipid oxidation
Mineral elements
Meat color
Myoglobin derivatives

ABSTRACT

Dry aging enhances beef's sensory quality, but the role of trace-element dynamics in driving physicochemical changes remains unclear. We dry-aged *Longissimus lumborum* loins (n = 12) for 60 days, sampling on days 1, 14, 35 and 60. Essential (Ca, K, Na, Mg, Fe, Se, Cr, Zn, Cu) and toxic (As, Cd, Co, Pb) elements were quantified by GF-AAS/FAAS; pH and L*, a*, b* color were measured with standard probes; lipid oxidation was assessed via TBARS; and myoglobin redox forms were determined spectrophotometrically. Inner muscle consistently retained higher K, Na, Mg, Zn, Cu and Cr compared to the crust ($P < 0.01$), reflecting diffusive retention during surface desiccation. Over 60 days, Ca, K, Se and Cr increased ($P < 0.01$) while Na and Mg decreased ($P < 0.001$). Iron and zinc exhibited a biphasic pattern, declining to day 35 and rebounding by day 60. Lipid oxidation intensified but remained below sensory rancidity thresholds (TBARS increased from 0.25 ± 0.07 to 0.65 ± 0.33 mg MDA/kg in inner meat and from 0.79 ± 0.15 to 1.53 ± 0.36 mg MDA/kg in crust; $P < 0.001$), concurrent with a pH rise from 5.61 ± 0.09 to 5.80 ± 0.19 ($P < 0.001$) and declines of approximately 11 % in redness (a*) and 15 % in yellowness (b*) ($P < 0.01$). Principal component analysis identified an oxidation-mineral-color gradient (PC1, 30.8 % variance) and a myoglobin-redox axis (PC2, 20.4 %), underscoring mechanistic links between trace element fluctuations, lipid oxidation, and color stability. These results demonstrate that dry aging concentrate minerals and that shifts in Fe, Se, and Zn trajectories modulate oxidative stability, pH drift, and pigment transformations, shaping dry-aged beef color and overall quality.

1. Introduction

Dry aging is a traditional meat-preservation technique that enhances flavor, tenderness and juiciness by holding primal or subprimal cuts under precisely controlled temperature (0–4 °C), air velocity (0.2–0.8 m/s) and relative humidity (75–85 %) for several weeks (Dashdorj et al., 2016; Perry, 2012). During this period, endogenous proteases, principally μ- and m-calpains and lysosomal cathepsins, degrade key myofibrillar proteins, concentrating flavor precursors and weakening muscle fibers (Toldrá & Flores, 1998).

However, extended storage also brings oxidative challenges: lipid peroxidation and myoglobin oxidation can lead to off-flavors and discoloration (Fig. 1). Although higher ultimate pH initially favors oxymyoglobin (OxyMb) formation and a bright red hue, cumulative reactive oxygen species (ROS) production during aging ultimately drives metmyoglobin (MetMb) accumulation and color loss, eventually overriding the pH benefit (Faustman et al., 2010; Mancini & Hunt, 2005).

Beef's mineral content is well-characterized nutritionally (Pereira, Vicente, & dos, 2013), but trace elements also modulate meat quality by participating in redox reactions (Patel et al., 2019). Trace elements such

* Corresponding author. CECAV—Centre for Studies in Animal and Veterinary Science, University of Trás-Os-Montes and Alto Douro (UTAD), Vila Real, Portugal.
E-mail addresses: anajacinta83@gmail.com, anaribeiro@utad.pt (A.J. Ribeiro), fbraga@utad.pt (F.G. Braga), ioliveir@utad.pt (I. Oliveira), fsilva@utad.pt (F. Silva), pcteixeira@ucp.pt (P. Teixeira), crisarai@utad.pt (C.M. Saraiva).

https://doi.org/10.1016/j.lwt.2025.118299
Received 4 June 2025; Received in revised form 5 August 2025; Accepted 6 August 2025
Available online 7 August 2025

as iron (Fe), zinc (Zn), copper (Cu) and selenium (Se) play pivotal roles in these redox processes. Fe catalyzes Fenton reactions, accelerating lipid and pigment oxidation (Min & Ahn, 2005), while Zn contributes to membrane stabilization and can inhibit free-radical chain reactions (Amaral et al., 2018). Cu acts as a cofactor for superoxide dismutase (Cu/Zn–SOD), converting superoxide radicals to hydrogen peroxide (Blanco-Penedo et al., 2010), and Se, as the catalytic core of glutathione peroxidase (GPx), reduces hydrogen and lipid hydroperoxides to non-radical products (Ramos et al., 2012; Zhang et al., 2020).

Despite extensive work on dry aging and on mineral nutrition individually, little is known about how shifts in tissue mineral profiles during aging impact the balance between proteolysis, lipid oxidation, and myoglobin chemistry and thus overall meat quality. Previous reviews have highlighted the importance of trace elements in muscle redox balance but have not examined their dynamic changes during dry aging (Chen et al., 2024; Silva et al., 2022).

The present study therefore set out to quantify both essential elements - calcium (Ca), potassium (K), sodium (Na), magnesium (Mg), selenium (Se), zinc (Zn), iron (Fe), copper (Cu) and chromium (Cr) - and toxic elements - arsenic (As), lead (Pb), cobalt (Co) and cadmium (Cd), element concentrations in the crust and inner meat of beef loins over 60 days of dry aging. Concurrently, lipid oxidation (TBARS), myoglobin redox forms (OxyMb, MetMb, DeoMb), color parameters (L*, a*, b*) and pH were measured to elucidate how trace element fluctuations influence oxidative stability and color development. By integrating mineral dynamics with proteolytic and oxidative markers, this work aims to clarify the mechanisms by which aging-driven mineral changes shape dry aged beef quality (Fig. 1).

2. Material and methods

2.1. Study design

This study was carried out in a Portuguese company certified for bovine dry aging, with no interference in its routine production protocols, in order to reflect the current practices for this process. Twelve loins *(Longissimus lumborum)* were selected from six animals with consistent characteristics: females, 5–8 years old, Portuguese breeds and crossbreeds, born and raised in a semi-extensive livestock production system in Portugal and slaughtered at same location and time. Each loin was divided into three pieces of approximately 5 kg, which were coded as duplicates for each animal (A/AZ; B/BZ; C/CZ; etc.), ensuring that all loins were included in each time point analysis. The pieces were placed horizontally in the dry-aging chamber, with the cut surface facing upward, so that each sampling time point (days 1, 14, 35, and 60) corresponded exactly to the intended aging. As aging progressed, the external surface became browner and drier and formed the characteristic crust (Fig. 2A and B). The first day of dry aging (day 1) was defined as the moment when the loin pieces entered the dry aging chamber (about three days after the meat arrived from the slaughterhouse). At the end of each time point analysis, the pieces used for sampling were coded (Animal code; time), separated from the remaining samples, and discharged at the end of the study.

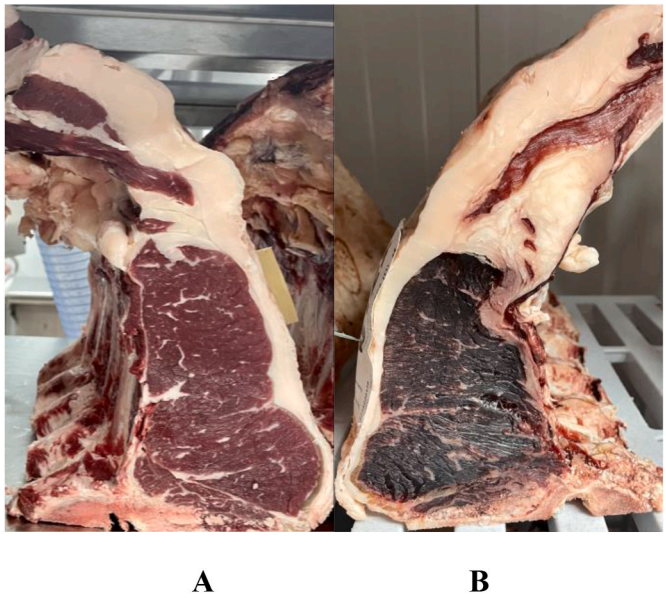

Fig. 2. Loin piece at (A) beginning (day 1) of dry aging study and at day 35 (B).

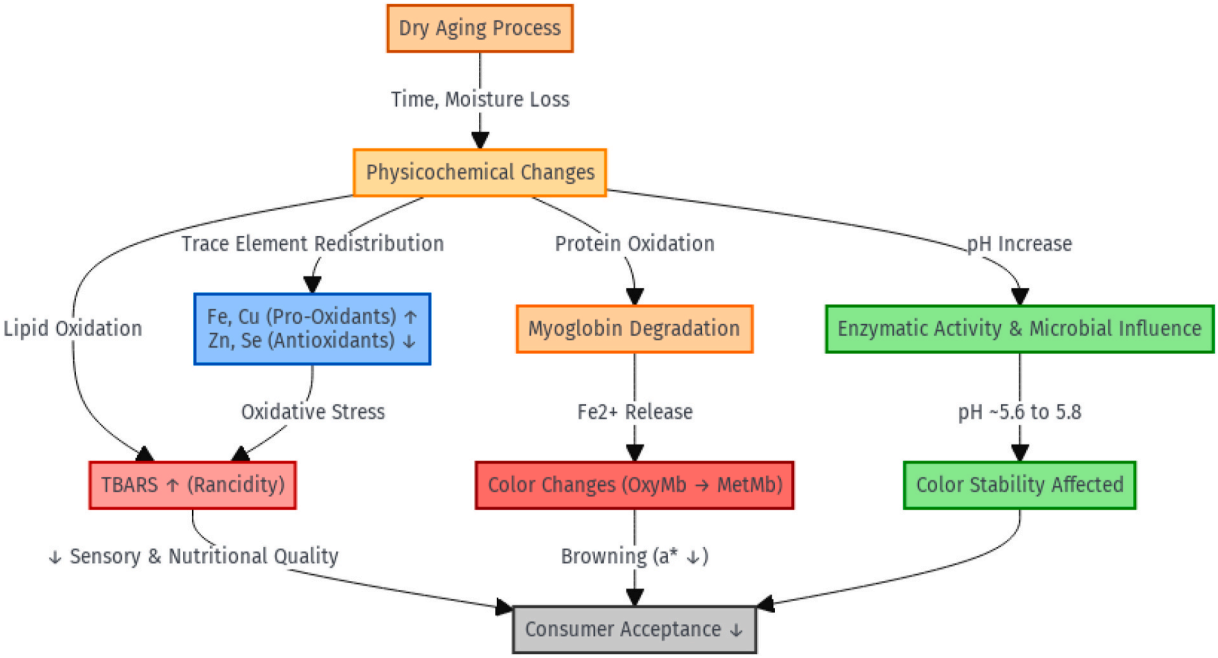

Fig. 1. Physicochemical changes and quality implications in dry aged beef.

2.2. Dry aged process guidelines

Dry aging was performed in certified storage chambers under the company's standard protocols, without any modifications. Internal conditions were totally controlled by the company maintained at a setpoint of 3 °C ± 1 °C and 60 % ± 10 % relative humidity (RH), monitored continuously with calibrated data loggers and probes data logging every 30 min. Air circulation (0.5–2.0 m/s at the meat surface) was provided by the chamber's ventilation system and periodically verified with a handheld anemometer. Ultraviolet A (UV-A) illumination was supplied by lamps integrated into the chamber ceiling, operating continuously to control surface microbial growth. Throughout the study, the temperature and RH in the dry aging chamber ranged from 4.3 °C to 2.1 °C and 69.0 %–55.4 %, respectively. Airflow was maintained within a programmed range of 0.5 m/s to 2.0 m/s.

2.3. Sample collection

On days 1, 14, 35 and 60 of the dry aging, one piece of each coded loin (total 12) was randomly selected and the intramuscular pH was measured. Subsequently, one hygienically excised sample was taken from the cut surface of each loin piece (total of 12). Each sample measured approximately 5 cm in thickness and weighed ~400 g (like a steak). The samples were transported to the laboratory at 4 °C within 1 h 30 min of excision. Upon arrival, samples were trimmed to simulate commercial dry aging practices: the external, non-edible layer (crust) was removed, revealing the inner, edible muscle located approximately 1 cm beneath the surface. Subsampling of both crust and inner muscle was performed according to the protocol of Capouya, Mitchell, Clark, Clark, and Bass (2020), with minor modifications. From each crust and inner meat, three 1 cm^3 sections of crust (totaling 3 × 10 g) and three 1 cm^3 sections of inner muscle (3 × 10 g) were collected. The three cubes from each tissue type were then randomly allocated among the assays: TBARS, myoglobin derivatives, mineral content, and (for inner muscle only) color L*a*b* color, to ensure unbiased, balanced representation. A total of 24 subsamples per time point (12 crust, 12 inner) were immediately processed for TBARS and myoglobin derivative analyses, while an additional 24 subsamples were vacuum-packaged and stored at −18 °C for mineral content determination. Quantification of myoglobin fractions, color L*a*b*, and pH was conducted exclusively on the inner muscle subsamples (n = 12 per time point).

2.4. Physicochemical analysis

Color and pH determinations were performed on the day of sample collection and only on meat samples (12 per time point), as it represents the marketable edible portion. Meat color was measured using a CR400 colorimeter (Konica Minolta Co., Tokyo, Japan) with CIE standard illuminant C as the light source, a 2° observer angle, and an 8 mm aperture diameter, calibrated with a standard white tile. L* (lightness), a* (redness), and b* (yellowness) values were measured at three random locations per sample. The intramuscular pH was measured using a portable HI98163 pH meter (Hanna Instruments, Woonsocket, RI, USA) with an FC2323 meat pH electrode and a stainless steel piercing blade (FC099). Prior to sample analysis, the instrument was calibrated using standard buffer solutions (at pH 4.01 and 7.01) at room temperature. Both the pH meter and the electrode featured automatic temperature compensation to ensure accurate pH readings despite minor temperature fluctuations during measurement.

2.5. Mineral analysis

The quantification of various minerals was performed in triplicate after digesting approximately 0.5 g of each sample with 65 % nitric acid and 30 % hydrogen peroxide (Merck, Darmstadt, Germany), following the procedure described by Patel et al. (2019), with the modification that we used flame atomic absorption spectrometry (FAAS) with an iCE 3000 Series instrument (Thermo Scientific, Cambridge, UK) for the determination of magnesium, calcium, potassium, iron, and sodium. Graphite furnace atomic absorption spectrometry (GF-AAS) was used for the analysis of zinc, chromium, copper, cobalt (Co), cadmium (Cd), arsenic (As), and lead (Pb), using a 939 AAS instrument equipped with a GF 90 Furnace and FS 90 Furnace Autosampler (Unicam, Cambridge, UK). Mineral content was expressed in mg/100 g of dry matter.

2.6. Selenium analysis

Samples were digested with 65 % nitric acid and 30 % hydrogen peroxide (Merck, Darmstadt, Germany) following AOAC International (1996) for selenium determination, with modifications introduced by Juszczak-Czasnojć et al. (2023), as described in subsection 2.3, and analyzed in triplicate. After cooling, the digested samples were diluted with ultrapure water to a final volume of 10 mL. Selenium was reduced to selenite (Se (IV)) by gentle heating at 90 °C for 30 min with concentrated hydrochloric acid (Merck, Darmstadt, Germany). After cooling, the selenite samples were derivatized with 2,3-diaminonaphthalene (DAN, Sigma-Aldrich, St. Louis, MO, USA) in a hydrochloric acid medium. The reaction mixtures were incubated for 60 min at room temperature in the absence of light. After extraction with cyclohexane, fluorescence intensity was measured at excitation and emission wavelengths of 370 nm and 520 nm, respectively, using a Cary Eclipse fluorescence spectrometer (Varian, Mulgrave, VIC, Australia). Selenium concentrations in the beef samples were determined by interpolating fluorescence intensities on a calibration curve. Method validation was performed using certified reference materials, spiked samples, and replicate analyses to assess accuracy, precision, and sensitivity. Selenium content was expressed in μg/100g of dry matter.

2.7. Quantification of myoglobin fractions

Myoglobin fractions were quantified using a GENESYS 50 UV–Vis (Thermo Scientific, Waltham, MA, USA) using the method described by Krzywicki (1979), modified by Suman and Joseph (2013). For each thawed meat sample (1.5 g), 4.0 mL of pH 6.8 phosphate buffer was added, and the mixture was homogenized for 5 min until uniform. The homogenate was centrifuged at 5500 rpm for 15 min at 4 °C. The absorbance of the clarified supernatants was measured at 525 nm, 545 nm, 565 nm, and 572 nm. Krzywicki's equations were used to determine the relative concentrations of DeoMb, OxyMb and MetMb based on their characteristic absorbance peaks.

2.8. Thiobarbituric acid reactive substances (TBARS) determination

Lipid oxidation was assessed following the method described by Ahn et al. (1998), with some modifications. Approximately 5 g of each sample (crust and lean meat) was homogenized with 20 mL of 5 % BioXtra trichloroacetic acid (Merck, Darmstadt, Germany) using an T 25 mini control ultra-turrax homogenizer (IKA-Werke GmbH & Co. KG, Staufen, Germany) at 13800 rpm for 1.5 min. The homogenate was centrifuged at 4000 g for 5 min, and the supernatant was filtered and adjusted to a final volume of 25 mL with 5 % TCA. Then, 2 mL of each sample solution was mixed with 2 mL of a 0.08 M 2-thiobarbituric acid (Merck, Darmstadt, German). The mixtures were incubated at 95 °C for 5 min, then cooled, vortexed, and centrifuged at 3000 g for 15 min. The absorbance of the supernatant was determined at 532 nm against a blank composed of 2 mL of 5 % TCA and 2 mL of 0.08 M TBA. TBARS concentrations were expressed as milligrams of malondialdehyde (MDA) per kilogram of meat.

2.9. Statistical analysis

To evaluate the effects of aging time and tissue location (crust vs.

meat) on essential element concentrations, TBARS values, pH, color parameters, and myoglobin redox forms, linear mixed-effects models were fitted using R (version 4.3.0) with the lme4 package. For variables measured in both tissue types (Ca, K, Na, Mg, Se, Zn, Fe, Cu, Cr, and TBARS), the models included aging time, tissue type, and their interaction as fixed effects. Loin, nested within animal (Loin:Animal), was treated as a random effect to account for repeated measures within individual carcasses. The general model structure for these variables was: **Y ~ Time + Tissue + Time:Tissue + (1 | Animal:Loin)**. For traits measured only in meat (color: L*, a*, b*, pH, and myoglobin derivatives: DeoMb, OxyMb, and MetMb), linear mixed-effects models with loin nested within animal, as random effect, were also used, but these models did not include the tissue or interaction terms. Where convergence issues occurred, models were simplified and these adjustments were indicated by superscript symbol. The model for these traits was: **Y ~ Time + (1 | Animal:Loin).**

Model fit was assessed using the Akaike Information Criterion (AIC). Fixed-effect significance was assessed via Type III Wald χ^2 tests and, when $P < 0.05$, pairwise comparisons among aging times were performed using emmeans with Tukey adjustment. Superscript letters indicate significant differences only when the Time × Tissue interaction was non-significant, otherwise differences were interpreted directly from model contrasts. Pearson correlation coefficients were calculated separately at each aging time point (days 1, 14, 35 and 60) to assess pairwise associations among trace elements, TBARS, pH, color parameters, and myoglobin forms. To avoid the misuse of pooled correlations on repeated-measures data, we applied repeated-measures correlation (rmcorr package in R) to estimate overall within-loin associations across all time points. The rmcorr analysis yielded the common within-subject correlation coefficient (r_rm) and its *P*-value. Significant correlations ($P < 0.05$) are shown in **bold.** Principal component analysis (PCA) was conducted in MetaboAnalyst 6.0 (Chong et al., 2019) and additionally replicated in R (version 4.3.0) using the FactoMineR package with autoscaling.

Prior to PCA, all variables (trace elements, TBARS, pH, color, and myoglobin derivatives) were log-transformed and unit-variance scaled. Pairwise Pearson correlations among all traits across the four aging times were then computed, and any variable exhibiting weak or nonsignificant associations ($|r| < 0.3$ or $P > 0.05$) with the majority of other measures was excluded to reduce analytical noise. Accordingly, DeoMb, Cu, Mg and L* were removed from the dataset. The remaining variables were subjected to PCA, and the first four principal components, explaining approximately 76.8 % of total variance, were retained. PCA scores, loadings, and biplots were exported from MetaboAnalyst and cross-checked against FactoMineR outputs to ensure consistency in the visualization and interpretation of multivariate relationships across the four aging time points.

3. Results and discussion

3.1. Changes in trace element concentrations and their implications

Dry aged trace element levels (values expressed on a dry matter basis) changed dynamically over time and, mostly, differed between crust and inner meat (Table 1). Moreover, mixed-effects modeling also identified significant time × tissue interactions for Mg and Zn ($P < 0.05$), indicating that their temporal profiles diverged between the tissues.

Furthermore, compared to previous reports, the overall mean values for Na, Mg, and Ca align closely with those of Campo et al. (2024) and Patel et al. (2019), whereas Cr, Fe, Cu, and Zn were lower. Such variability confirms the influence of intrinsic factors identified by other authors, such as breed (Litwińczuk et al., 2015; Pereira et al., 2013; Pilarczyk, 2014), age (Patel et al., 2020), and production system, on mineral deposition. This study was designed with Portuguese autochthonous crossbreed cows (5 years old) reared semi-extensively which can provide a novel context for evaluating how these factors modulate baseline trace element levels prior to aging.

Inner meat showed significantly higher levels of K, Na, Mg, Zn, Cu and Cr than crust ($P < 0.01$), consistent with inward diffusion driven by moisture and solute concentration gradients during surface desiccation (Yu et al., 2024; Álvarez et al., 2021). By contrast, Ca, Se, and Fe showed no tissue differences ($P > 0.05$), suggesting strong binding to myofibrillar proteins or slower leaching kinetics under the controlled low humidity conditions used (Koohmaraie & Geesink, 2006).

Over the full aging period, Ca, K, Se, Zn, Fe, and Cr increased overall ($P < 0.05$), while Na and Mg declined sharply ($P < 0.001$) and Cu decreased modestly ($P > 0.05$). Notably, Zn, Fe, and Cr each exhibited a biphasic pattern: they declined from day 1 to day 35 before rebounding by day 60. During the initial phase (days 1–35), labile metal pools, including free Fe, loosely bound Zn, and Cr - peptide complexes, diffused into purge fluid, resulting in net losses in both crust and inner muscle (Amaral et al., 2018; Min & Ahn, 2005). Concurrently, progressive surface dehydration between days 14 and 35 formed a semipermeable pellicle that significantly reduced further exudation (Álvarez et al., 2021). From day 35 onward, sustained proteolytic activity, driven by μ and m-calpains and lysosomal cathepsins, cleaved metalloproteins and heme-containing proteins, releasing Zn, Fe, and Cr back into the tissue matrix. Ongoing moisture loss then concentrated these liberated ions, producing the late-aging rebound in their measured levels (Domínguez et al., 2019; Faustman et al., 2010).

Although, the present study did not quantify heme-bound versus non-heme Fe, and thus, without speciation data, the precise balance between free and protein-bound iron remains uncertain, the observed changes in iron and its role in oxidative stability are discussed in section 3.2.

Table 1
Main and interaction effects of aging time and tissue type (means ± se, mg/100g and μga/100g, in dry matter basis) obtained from mixed-effects models for each mineral and quality trait.

Parameters	Tissue			Aging Time					Time x tissue
	Crust	Meat	*P* value	1	14	35	60	*P* value	*P* value
Ca	4.40 ± 6.21	4.31 ± 4.43	0.919	3.65 ± 2.39	1.66 ± 1.46	2.50 ± 2.14	9.60 ± 8.12	<0.001	0.870
K	648.46 ± 330.68	1093.44 ± 292.74	<0.001	723.01 ± 309.33	1001.32 ± 378.46	896.05 ± 478.39	863.43 ± 310.04	0.007	0.209
Na¤	246.20 ± 129.58	361.70 ± 162.03	<0.001	314.71 ± 200.06	333.53 ± 87.01	359.09 ± 120.97	208.48 ± 161.03	<0.001	0.854
Mg	7.37 ± 2.77	10.11 ± 2.95	<0.001	10.35 ± 4.08	7.36 ± 1.92	8.88 ± 3.20	8.37 ± 2.41	<0.001	0.005
Se¤[a]	5.99 ± 4.92	8.91 ± 4.87	0.501	5.18 ± 1.81	6.94 ± 4.97	6.30 ± 2.92	11.37 ± 6.87	<0.001	0.095
Zn	8.57 ± 4.59	17.24 ± 8.56	<0.001	13.01 ± 6.96	10.91 ± 4.41	11.14 ± 4.76	16.56 ± 12.63	0.002	<0.001
Fe¤	6.52 ± 5.56	7.80 ± 3.77	0.601	8.05 ± 6.72	6.15 ± 2.76	5.89 ± 3.74	8.55 ± 4.65	0.048	0.354
Cu	0.99 ± 0.61	1.80 ± 0.71	<0.001	1.43 ± 0.65	1.58 ± 0.89	1.43 ± 0.89	1.14 ± 0.62	0.095	0.132
Cr¤	0.21 ± 0.21	0.30 ± 0.26	0.002	0.27 ± 0.23	0.16 ± 0.15	0.11 ± 0.05	0.47 ± 0.29	<0.001	0.154
TBARS¤	1.03 ± 0.38	0.39 ± 0.24	<0.001	0.52 ± 0.30	0.55 ± 0.31	0.67 ± 0.35	1.09 ± 0.56	<0.001	<0.001

Crust – exterior surface of the beef; Meat – interior part of the beef; ¤Models simplified.

Copper serves as a cofactor for Cu/Zn–superoxide dismutase (SOD); its depletion implies reduced SOD activity over time. Indeed, progressive Cu loss correlated with increasing TBARS values, reinforcing Cu's role in modulating oxidative stress (Silva et al., 2022). Lower Cu reduces enzymatic quenching of superoxide radicals, thereby permitting greater lipid peroxidation (Amaral et al., 2018).

Ca and K concentrations rose steadily from day 1 through day 60, suggesting water loss from muscle fibers (Domínguez et al., 2019). Elevated Ca^{2+} enhances calpain activity, driving proteolysis and contributing to tenderization during aging, as demonstrated by Kim et al. (2018).

Magnesium and zinc showed significant tissue x time effects ($P < 0.05$). For Mg, the significant divergence is shown in Fig. 3A, where the concentrations on inner meat fell from 13.19 ± 3.08 mg/100 g (day 1) to 8.74 ± 1.59 mg/100 g (day 14) ($P < 0.05$) and remained lower through day 60. Early in aging, intracellular Mg, largely complexed to ATP and ribosomal RNA, becomes mobile as ATP degrades, diffusing into exudate and is carried away (Khan et al., 2016).

Zinc also showed higher means in inner meat comparing to the crust ($P < 0.001$) and changed significantly over aging time ($P < 0.05$). Meat levels decreased from 17.22 ± 6.74 mg/100 g (day 1) to 12.32 ± 2.54 mg/100 g (day 35), then significantly surged to 25.95 ± 10.72 mg/100 g (day 60) (Fig. 3B). After initial leaching, profound proteolysis of Zn-rich myofibrillar and metalloproteins (e.g., carbonic anhydrase, metallothioneins) liberates Zn into the tissue, and moisture loss concentrates it (Khan et al., 2016). High Zn in late-aged inner muscle may be actively complexed by upregulated metallothioneins, which scavenge free radicals (Amaral et al., 2018; Mocchegiani et al., 2000). In contrast, crust levels of Zn and Mg declined steadily, from 8.79 ± 4.11 mg/100 g (day 1) to 7.18 ± 5.13 mg/100 g (day 60) for Zn, and from 7.60 ± 2.98 mg/100 g (day1) to 7.91 ± 2.06 mg/100 g (day 60) for Mg. Surface drying forms a semipermeable pellicle, limiting exudation and preserving mineral levels in the crust (Álvarez et al., 2021).

In this study, toxic elements such as Cd, As and Pb were below detection limits (Cd < 0.005 μg/L; As < 0.010 μg/L; Pb < 0.020 μg/L), consistent with research indicating that controlled livestock environments minimize toxic metal contamination (Blanco-Penedo et al., 2010). This is critical for ensuring the safety and regulatory compliance of dry aged meat products.

3.2. Lipid oxidation progression and its impact on meat quality

Lipid oxidation, assessed by TBARS, increased steadily over the 60-day dry-aging period, with a pronounced **time** × **tissue** interaction ($P < 0.001$; Fig. 3C). From an initial value of 0.79 ± 0.15 mg MDA/kg in the crust versus 0.25 ± 0.07 mg MDA/kg in the inner muscle (day 1), oxidation progressed more rapidly in the crust, reaching 1.53 ± 0.35 mg MDA/kg by day 60, compared to 0.65 ± 0.33 mg MDA/kg in the interior ($P < 0.05$). Accelerated peroxidation at the surface reflects greater oxygen availability and may be exacerbated by UV-induced ROS generation during microbial control (Amaral et al., 2018; Kim et al., 2016; Xue et al., 2021).

Even though TBARS remained below the 2.0 mg MDA/kg threshold for sensory rancidity (Campo et al., 2006), subthreshold oxidation can still affect color via reactive aldehydes like malondialdehyde and 4-hydroxynonenal. These aldehydes promote heme-iron oxidation, weakening pigment binding and accelerating MetMb formation (Faustman et al., 2010; Han et al., 2024).

Mechanistically, lipid peroxidation follows a free-radical chain reaction: initiation by •OH or ROO• radicals, propagation (via hydrogen abstraction from unsaturated lipids), and termination (when radicals combine). Transition metals exacerbate propagation — the Fenton reaction ($Fe^{2+} + H_2O_2 \rightarrow Fe^{3+} + \bullet OH + OH^-$) and Cu-catalyzed hydroperoxide cleavage both generate RO• and ROO• species that further oxidize lipids and pigments (Faustman et al., 2010). In this study, total Fe decreased through day 35 before rebounding by day 60 (Table 1), reflecting proteolytic release from heme proteins and transient ferritin sequestration (Min & Ahn, 2005). The rise in free Fe likely accelerated OxyMb to MetMb conversion, consistent with the sharper a* decline observed after day 35 (Amaral et alAmaral et al., 2018; Domínguez et al., 2019).

3.3. Myoglobin redox forms, color stability and pH regulation

Color attributes also changed significantly over time (Table 2). **Lightness (L*)** decreased slightly, while **redness (a*)** and **yellowness (b*)** both declined significantly ($P < 0.01$), indicating progressive discoloration, especially during the later aging stage (35–60 days). Myoglobin derivatives equilibrated during aging, with OxyMb declining significantly at day 14 and then stabilizing. The transient mid-aging peak in MetMb, followed by a modest decline, reflects early oxidative activity countered by antioxidant defenses and pH buffering.

Similar myoglobin oxidation kinetics, featuring initial MetMb rise followed by partial reduction, have been documented (Faustman et al., 2010; Mancini & Hunt, 2005). Additionally, proteolysis-driven pH increases may enhance MetMb-reductase activity, contributing to MetMb reduction after the initial peak (Ribeiro et al., 2021a, 2021b). These trends and the fluctuations in iron concentrations are consistent with Fe

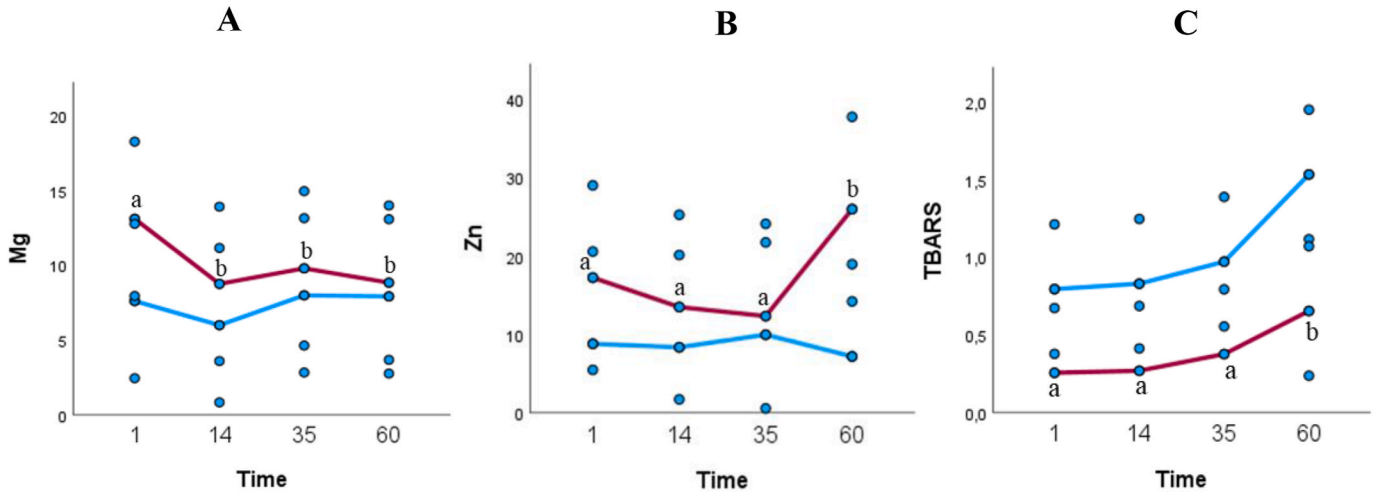

Fig. 3. Magnesium (A), zinc (B) and TBARS (C) distribution on crust (blue line) and inner meat (red line) during dry aging time. Different letters (a and b), along each line indicate significantly differences ($P < 0.05$).

Table 2
Physicochemical variables (means ± SE) of the interior of the strip loins (*Longuissimus lumborum*), on days 1, 14, 35 and 60 of dry aging.

Parameters	Aging time				*P*-value
	1 d	14 d	35 d	60 d	
L*	35.1 ± 4.2	36.1 ± 1.7	35.4 ± 1.9	34.3 ± 3.0	0.477
a*	24.4 ± 1.8^{a}	24.4 ± 1.2^{a}	22.7 ± 2.2^{ab}	21.8 ± 3.5^{b}	0.009
b*	14.2 ± 1.0^{a}	13.8 ± 1.5^{ab}	12.6 ± 1.4^{bc}	12.1 ± 1.6^{c}	<0.001
DeoMb	0.09 ± 0.03	0.10 ± 0.07	0.08 ± 0.03	0.08 ± 0.03	0.695
OxyMb	0.57 ± 0.06	0.49 ± 0.12	0.54 ± 0.08	0.53 ± 0.12	0.125
MetMb	0.31 ± 0.03	0.36 ± 0.13	0.32 ± 0.09	0.33 ± 0.12	0.429
pH	5.61 ± 0.09^{a}	5.73 ± 0.11^{ab}	5.86 ± 0.13^{c}	5.80 ± 0.19^{bc}	<0.001

Values with different superscripts ($^{a, b, c}$) in the same row differ significantly ($P < 0.05$).

and Cu catalyzing myoglobin oxidation and MetMb formation (Faustman et al., 2010). The gradual increase in pH, from ~5.6 (day 1) to 5.8 (day 60), can stabilize myoglobin and delay pigment oxidation (Ribeiro, Lau, Pflanzer, et al., 2021). Slightly more alkaline conditions raise the redox potential of the myoglobin system and enhance metmyoglobin-reductase activity, reconverting of MetMb to OxyMb and postponing discoloration (Mancini & Hunt, 2005). This pH-driven color stability has also been observed in high-pH beef, where elevated muscle pH correlates with slower MetMb accumulation and prolonged redness (Ramanathan et al., 2019). Proteolysis and enzymatic reactions during aging release basic amino groups, contributing to the pH rise. This shift, alongside with crust desiccation and UV sanitation, supports oxidative stability and microbial control (Monteiro et al., 2023; Ramanathan et al., 2020; Ribeiro et al., 2023).

3.4. Principal components analysis and correlations

The PCA was conducted on a subset of variables that showed meaningful interrelationships and biological relevance to dry-aging dynamics: essential minerals (Ca, Se, Zn, Fe), color coordinates (a* and b*), myoglobin redox forms (OxyMb and MetMb), TBARS, and pH. Magnesium, copper, lightness (L*) and deoxymyoglobin (DeoMb) were excluded because each exhibited weak pairwise correlations ($|r| < 0.30$) or non-significant associations ($P > 0.05$) with the retained variables, indicating they would contribute little to the principal component structure and might introduce noise rather than clarify the underlying data patterns.

The analysis extracted four dimensions explaining approximately 76.8 % of the total variance (Fig. 4) and all variables are well explained with these 4 axes. The lowest communality value was 0.486 from pH, indicating that most variables were well explained by the extracted dimensions (Table 3). The PCA likely allowed the differentiation of samples according to aging time (colored shading). Early aging stages (day 1 and 14) clustered together, characterized by relatively lower TBARS values, more stable myoglobin forms (i.e., higher OxyMb) and lower concentrations of certain trace elements. In contrast, later stages (day 35 and 60) would shift towards higher TBARS values and concentrated mineral levels due to moisture loss. Such differentiation reinforces that aging not only alters individual parameters but also transforms the overall interrelationship between oxidative processes, trace element dynamics and meat quality attributes (Dragoev, 2024; Ribeiro, Lau, Furbeck, et al., 2021).

The first principal component (Dim1 – 30.8 %) likely captures the primary variation related to oxidation processes and mineral concentration. The strong positive loading of TBARS suggests that this

Table 3
Proportion of variance explained (communalities) for each trait in the four dimensions.

Traits	Dim1	Dim2	Dim3	Dim4	Communality
Ca	0.391	0.5074	0.6045	−0.01794	0.776
Se	0.643	−0.0474	−0.1120	0.54151	0.722
Zn	0.015	0.4462	0.7848	−0.01224	0.815
Fe	0.488	−0.3320	0.2114	0.55403	0.700
a*	−0.687	−0.2495	0.1137	0.40742	0.713
b*	−0.695	−0.2592	0.1790	0.47217	0.805
OxyMB	−0.287	0.8271	−0.2736	0.23223	0.895
MetMb	0.152	−0.8080	0.3295	−0.32575	0.891
TBARS	0.928	−0.0499	0.0044	0.12775	0.880
pH	0.600	0.0702	−0.3482	−0.00987	0.486

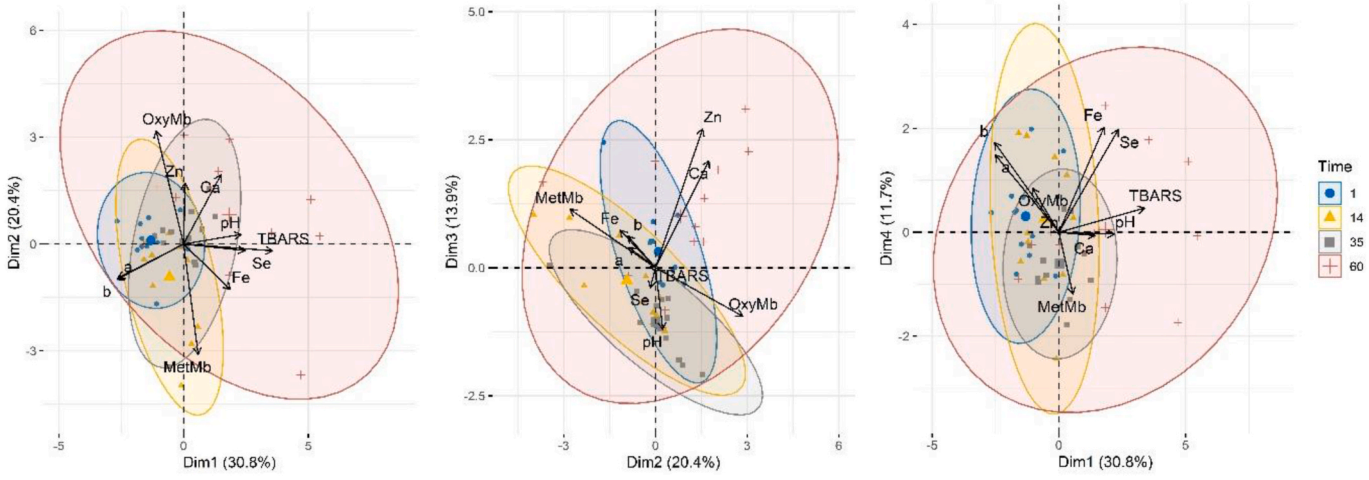

Fig. 4. Principal components analysis (PCA) biplots illustrating the physicochemical variables: essential elements (Ca, Se, Zn, Fe), color attributes (a* and b*), myoglobin redox forms (OxyMb and MetMb) and TBARS. Different samples are differentiated by aging time: 1 day is represented by blue shading (circles), 14 days by yellow shading (triangles), 35 days by brown shading (squares) and 60 days by red shading (crosses).

dimension strongly reflects lipid oxidation intensity (Fig. 4). This component loads positively on TBARS, Fe, Se and pH and negatively on a* and b*, capturing the shift from fresh to oxidized status (Domínguez et al., 2019; Huff-Lonergan & Lonergan, 2005). Higher TBARS and Fe concentrations reflect intensified lipid peroxidation catalyzed by free iron (Faustman et al., 2010), while declining a* and b* indicate color degradation (Min & Ahn, 2005). Early samples (days 1–14) score negatively on Dim 1 (lower TBARS, higher redness), whereas late samples (days 35–60) migrate positively as TBARS rise.

The second principal component (Dim2 - 20.4 %) likely represents the oxidation states of myoglobin. The high positive loading of OxyMb, combined with the similarly high but opposite loading of MetMb, indicates that this dimension reflects the myoglobin redox balance. This redox shift is crucial for maintaining the bright red color of meat. The contribution of color parameters further confirms that Dim2 is closely related to visual meat quality, as the shift from OxyMb to MetMb is associated with browning and discoloration (Ribeiro, Lau, Pflanzer, et al., 2021).

The third principal component (Dim3 – 13.9 %) likely reflects changes associated with moisture loss and mineral concentration shifts. As aging progresses, the concentrations of essential elements such as Zn and to some extent, Ca increase due to dehydration and the enzymatic breakdown of muscle proteins. Thus, Dim3 can be interpreted as an axis of nutrient concentration changes resulting from the aging process. This separation highlights how water loss during dry aging concentrates these minerals in lean meat, affecting pH and indirectly, color stability (Ramos et al., 2012).

The fourth principal component (Dim4 – 11.7 %) captures a more nuanced variation that is less dominant than the first three dimensions. The positive loadings for Se and Fe suggest that this dimension reflects additional variability in trace element profiles, potentially linked to antioxidant defenses (Se) and continued iron dynamics beyond the primary oxidative effects observed in Dim1. Although its overall contribution to the explained variance is lower, Dim4 may still play a role in fine-tuning the understanding of how subtle shifts in trace element composition influence color stability and oxidation processes (Chen et al., 2024).

The Pearson correlation matrix (Fig. 5) shows that TBARS correlates positively with Ca ($r = 0.425$), Se ($r = 0.589$), and Fe ($r = 0.473$), and negatively with redness (a*) ($r = -0.575$) and yellowness (b*) ($r = -0.644$), highlighting how pro-oxidant iron and the antioxidant trace element selenium together influence lipid oxidation and color loss during dry aging (Amaral et al., 2018). Interestingly, despite selenium's established role in antioxidant defenses, its positive correlation with TBARS in our data suggests a more complex relationship. For instance, Jung et al. (2024) found no effect of dietary selenium supplementation on pork TBARS values, underscoring that selenium's impact on lipid peroxidation may depend on its tissue speciation, cofactors, or the timing of its release during proteolysis (Jung et al., 2024). These discrepancies point to the need for targeted studies on selenium speciation and enzyme activity (e.g., GPx) in dry aged beef to unravel how selenium shifts from an antioxidant reservoir to a correlated marker of oxidative progression (Surai et al., 2019).

Muscle pH correlated moderately positively with lipid oxidation (TBARS; $r = 0.449$) and moderately negatively with yellowness (b*; $r = -0.423$), consistent with proteolysis-driven alkalinization that both enhances metmyoglobin-reductase activity transiently buffering oxidative stress and shifts the myoglobin equilibrium toward DeoMb at higher pH, yielding paler, less yellow meat (Domínguez et al., 2019; Huff-Lonergan & Lonergan, 2005). A strong positive correlation between redness (a*) and yellowness (b*) ($r = 0.686$) reflects the concurrent loss of both pigments as lipid peroxidation advances, since oxidative products accelerate metmyoglobin formation and pigment pigment degradation (Mancini & Hunt, 2005). Finally, the very strong inverse relationship between OxyMb and MetMb ($r \leq -0.85$) captures the classic red-to-brown transition driven by myoglobin oxidation on the meat surface (Faustman et al., 2010; Mancini & Hunt, 2005).

Fig. 5 also shows that at early aging stages (days 1–14), Zn and Mg exhibited an exceptionally strong positive correlation (day 14: $r = 0.922$), reflecting their intact intracellular pools and joint roles as cofactors for antioxidant enzymes, particularly Zn/Cu–superoxide dismutase and Mg-dependent metmyoglobin reductase, in agreement with the observations of Mancini and Hunt (2005) and Perry (2012). On day 1, Zn also correlated strongly with Fe ($r = 0.728$), which is consistent with the binding of iron within heme proteins and its involvement in early redox chemistry, supporting the previous observations of Faustman et al. (2010). By day 14, Mg–Cu ($r = 0.570$) and Zn–Cu ($r = 0.685$) remained significantly associated, highlighting copper's key function in SOD activity. Trace metals also tracked closely with deoxymyoglobin: Zn–DeoMb (day 14: $r = 0.819$) and Mg–DeoMb ($r = 0.940$), which aligns with high residual ATP and metmyoglobin-reductase activity reconverting MetMb to its reduced forms under minimal drip loss according to

	Ca		0.219		-0.064		**0.577**		0.000		-0.124		-0.200		**-0.326**		-0.269		-0.299		0.082		0.027		**0.425**		0.080
0.236	0.332		Se		**-0.388**		0.028		**0.382**		-0.233		-0.290		-0.242		-0.144		0.066		-0.255		0.024		**0.589**		0.228
0.088	-0.033																										
0.583	-0.123	-0.084	-0.389		Mg		-0.293		0.118		0.239		0.100		0.223		0.122		0.153		0.016		-0.024		**-0.153**		-0.275
0.435	0.286	0.383	0.243																								
-0.342	-0.196	-0.153	-0.344	-0.457	0.922		Zn		0.112		-0.100		-0.270		-0.166		-0.048		-0.157		0.221		-0.118		0.214		-0.009
0.130	0.386	0.166	-0.672	0.680	-0.449																						
-0.319	0.399	0.210	0.335	-0.239	-0.039	0.728	-0.007		Fe		0.063		-0.200		-0.102		-0.027		0.324		-0.087		-0.142		**0.473**		-0.034
0.249	-0.334	0.277	0.574	0.667	0.290	0.730	-0.696																				
-0.040	0.056	0.483	-0.373	0.081	0.57	0.118	0.685	0.414	0.011		Cu		0.150		-0.091		-0.297		0.265		-0.071		-0.075		-0.030		0.295
0.430	0.208	-0.460	-0.241	0.118	-0.093	0.239	0.090	0.383	-0.040																		
0.421	-0.224	0.308	-0.334	0.545	0.037	-0.390	0.072	0.022	-0.011	0.312	0.102		L*		**0.383**		0.180		-0.217		0.113		0.248		-0.231		0.180
-0.090	-0.295	-0.241	-0.770	-0.537	-0.118	-0.512	0.285	-0.550	-0.402	-0.044	0.088																
0.145	0.014	-0.060	0.401	-0.191	0.197	0.155	0.36	0.057	0.118	0.056	-0.06	0.461	-0.013		a*		**0.686**		-0.016		0.011		0.133		**-0.575**		-0.238
-0.202	-0.120	-0.113	-0.327	0.152	0.007	-0.077	0.229	0.255	-0.340	0.145	-0.533	0.215	0.622														
-0.502	0.375	-0.223	0.545	-0.471	-0.368	0.702	-0.312	0.574	0.292	0.167	-0.514	-0.031	-0.157	0.601	0.482		b*		-0.166		0.107		0.046		**-0.644**		**-0.423**
0.044	-0.116	-0.068	-0.391	0.326	-0.342	-0.193	0.411	0.072	-0.741	-0.111	-0.102	-0.203	0.646	0.478	0.655												
0.000	-0.069	0.029	-0.317	-0.403	0.94	0.380	0.819	0.258	-0.077	-0.048	0.546	-0.365	0.085	-0.038	0.192	0.208	-0.455	DeoMb		-0.291		-0.265		0.105		0.042	
-0.414	-0.448	-0.223	0.420	-0.159	0.243	0.305	-0.706	-0.183	0.748	-0.374	-0.347	-0.317	-0.018	-0.450	0.234	-0.162	-0.280										
0.339	-0.494	0.145	0.403	0.509	-0.279	-0.579	-0.117	-0.423	-0.082	0.165	-0.414	0.541	-0.134	0.031	0.366	-0.457	0.068	-0.796	-0.223	OxyMb		**-0.747**		-0.128		0.173	
0.274	0.318	0.237	-0.425	-0.005	-0.200	0.181	0.474	-0.069	-0.538	-0.032	0.481	-0.283	0.506	-0.860	0.276	-0.647	0.602	0.257	-0.455								
0.042	0.511	0.016	-0.135	-0.129	-0.325	0.536	-0.385	0.387	0.22	-0.135	0.048	-0.226	0.14	0.223	-0.46	0.414	0.204	0.093	-0.423	-0.518	-0.771	MetMb		-0.073		-0.251	
-0.250	-0.318	-0.175	-0.102	-0.083	0.110	-0.374	-0.129	-0.043	0.236	0.038	-0.244	0.477	-0.144	0.812	-0.238	0.508	-0.466	-0.521	0.127	-0.903	-0.825						
-0.385	0.409	-0.018	0.503	0.006	-0.542	0.196	-0.521	0.506	0.619	0.141	-0.181	-0.317	0.125	-0.645	-0.012	-0.066	0.279	0.160	-0.466	-0.407	-0.131	0.145	0.503	TBARS		**0.449**	
0.487	-0.273	0.224	0.778	0.238	0.306	-0.061	-0.764	0.144	0.880	-0.028	0.007	0.248	-0.652	0.051	-0.552	-0.080	-0.708	-0.509	0.535	-0.036	-0.545	0.276	0.161				
-0.075	0.161	0.368	-0.21	-0.018	0.092	-0.096	0.126	0.202	0.303	0.780	0.361	0.047	0.753	-0.089	0.029	-0.073	-0.172	0.083	0.247	0.004	-0.201	-0.170	0.076	0.208	0.231	pH	
0.281	-0.001	0.099	0.420	0.017	0.021	-0.225	-0.188	-0.010	0.527	-0.078	0.410	0.533	-0.301	0.198	-0.255	-0.222	-0.274	-0.468	0.176	-0.035	0.181	0.285	-0.351	0.742	0.518		

Fig. 5. Total and time-specific Pearson Correlation Matrices for dry-Aged beef quality traits. The upper triangle displays the overall (pooled) Pearson correlation coefficients among the measured traits, including trace elements, lipid oxidation (TBARS), myoglobin redox forms (OxyMb, MetMb, DeoMb), color parameters (L*, a* and b*) and pH, across all samples. The lower triangle is subdivided into four panels corresponding to individual aging times (day 1-top left square, day 14-top right square, day 35-low left square, and day 60-low right square), where each panel shows the partial correlations calculated only for that specific time point. Blue colors indicate positive correlations, while red colors represent negative correlations; the intensity reflects the strength of the association. Bolded values indicate statistically significant correlations with *P*-values <0.05.

Faustman et al. (2010). The strong positive correlation between redness (a*) and yellowness (b*) on day 1 (r = 0.601) further illustrates a low-oxidation, oxygen-rich surface environment observed by Domínguez et al. (2019). Conversely, the pronounced negative correlation between DeoMb and OxyMb at day 1 (r = −0.796) captures the rapid oxygen-binding equilibrium of myoglobin upon air exposure.

In the mid to late aging phase (days 35–60), trace-element interrelationships and oxidation markers intensified as dehydration and proteolysis concentrated minerals in the muscle. By day 60, Zn and Fe showed a strong inverse correlation (r = −0.696), suggesting that iron liberated from heme during proteolysis promotes oxidative loss of zinc's protective capacity. Selenium and iron were positively associated at day 60 (r = 0.574), reflecting concurrent mobilization of Se-dependent glutathione peroxidase with free iron to counteract rising ROS as proposed by Huff-Lonergan and Lonergan (2005) and Chen et al. (2024). The Zn–Mg link remained robust at day 35 (r = 0.680), driven by moisture loss concentrating both cofactors for metmyoglobin-reductase and carbonic anhydrase. Lipid oxidation (TBARS) correlated very strongly with Fe on day 60 (r = 0.880), confirming iron's catalytic role in Fenton chemistry, and inversely with b* (r = −0.708), indicating that advanced peroxidation depletes color pigments in accordance with Domínguez et al. (2019) observations. TBARS also correlated negatively with zinc (r = −0.764), showing Zn's diminishing antioxidant influence under excessive ROS. Muscle pH rose in parallel with TBARS at day 35 (r = 0.742) and with Fe at day 60 (r = 0.527), consistent with proteolysis-driven alkalinization that accelerates lipid oxidation and pigment oxidation kinetics.

4. Conclusion

Dry aging under controlled temperature and low humidity conditions elicits coordinated shifts in mineral composition, oxidation processes, and color attributes in beef over a 60-day period. Inner meat consistently retained higher levels of K, Na, Mg, Zn, Cu compared to the crust, aligning with moisture-driven diffusion gradients. Essential elements (Ca, K, Se) concentrated steadily due to dehydration, while Zn, Fe, and Cr exhibited a biphasic trend, declining through mid-aging (day 35) as labile pools leached, then rebounding by late aging (day 60) via proteolytic release and further moisture loss. Toxic elements (Cd, As, Pb) remained below detection limits, confirming product safety. Lipid oxidation (TBARS) increased most sharply in the crust but remained below sensory rancidity thresholds. The post-day-35 rise in total iron levels may contribute to the observed oxymyoglobin-to-metmyoglobin conversions, accompanied by declines in redness, yellowness, and lightness. A modest pH drift supported metmyoglobin-reductase activity, temporarily buffering discoloration, while proteolysis-derived peptides and low surface moisture helped maintain microbial stability. Principal components analysis distilled these dynamics: the primary axis captured the oxidation-mineral-color gradient (TBARS, Fe and Se versus a*, b*), and the second reflected OxyMb-MetMb balance. Additionally, correlation patterns mirrored the PCA-TBARS correlated positively with Fe and Se and negatively with a* and b*, while early aging featured strong Zn-Mg-OxyMb associations under low-oxidation conditions, which transitioned to TBARS–Fe and Se–Zn couplings as oxidative stress increased.

These findings suggest that dry aging increase beef minerals levels, which could enhance the meat's nutritional value. They also indicate that monitoring Zn, Se and Fe trajectories alongside TBARS and color metrics can guide optimal aging endpoints. Adjusting humidity and airflow to mitigate early mineral depletion, combined with mid-aging antioxidant interventions, may help preserve redness and quality. Future work should resolve mineral speciation, integrate protein oxidation and volatile profiling, and assess microbial and sensory outcomes to refine dry aging quality protocols.

CRediT authorship contribution statement

Ana J. Ribeiro: Writing – review & editing, Writing – original draft, Methodology, Investigation. **Fernando G. Braga:** Writing – review & editing, Methodology. **Irene Oliveira:** Methodology. **Filipe Silva:** Supervision. **Paula Teixeira:** Supervision. **Cristina M. Saraiva:** Supervision.

Funding

This work was supported by the projects UIDB/CVT/00772/2020 (DOI:10.54499/UIDB/00772/2020), LA/P/0059/2020, UIDB/00616/2020, UIDB/00616/2025, UIDB/04621/2025 of the Portuguese Science and Technology Foundation (FCT).

Declaration of competing interest

All authors declare that they have no conflict of interest in the subject matter or materials discussed in this manuscript. The authors have no financial interests, consultancy roles, or affiliations with companies or organizations that could be perceived to influence the content or conclusions of this study.

Acknowledgements

Ana J. Ribeiro, Cristina Saraiva and Filipe Silva would like to thank CECAV and AL4AnimalS and the support of the projects: UIDB/CVT/00772/2020 (DOI:10.54499/UIDB/00772/2020), LA/P/0059/2020 and UIDB/00616/2020, of the Portuguese Science and Technology Foundation (FCT). This work was also supported by the projects, UIDB/00616/2025 - Chemistry Research Center and UIDB/04621/2025 - CEMAT of the Portuguese Science and Technology Foundation (FCT). We also express our gratitude to Carlos Matos for performing the mineral analysis.

Data availability

Data will be made available on request.

References

Ahn, D. U., Olson, D. G., Jo, C., Chen, X., Wu, C., & Lee, J. I. (1998). Effect of muscle type, packaging, and irradiation on lipid oxidation, volatile production, and color in raw pork patties. *Meat Science, 49*(1), 27–39. https://doi.org/10.1016/s0309-1740(97)00101-0

Álvarez, S., Álvarez, C., Hamill, R., Mullen, A. M., & O'Neill, E. (2021). Drying dynamics of meat highlighting areas of relevance to dry-aging of beef. *Comprehensive Reviews in Food Science and Food Safety, 20*(6), 5370–5392. https://doi.org/10.1111/1541-4337.12845

Amaral, A. B., Solva, M. V. D., & Lannes, S. C. D. S. (2018). Lipid oxidation in meat: Mechanisms and protective factors - A review. *Food Science and Technology, 38*(1), 1–15. https://doi.org/10.1590/fst.32518

AOAC International. (1996). AOAC official method 974.15-1976: Selenium in human and pet food. Fluorometric method. In *Official methods of analysis of AOAC international* (16th ed.). AOAC International.

Blanco-Penedo, I., López-Alonso, M., Miranda, M., Hernández, J., Prieto, F., & Shore, R. F. (2010). Non-essential and essential trace element concentrations in meat from cattle reared under organic, intensive or conventional production systems. *Food Additives & Contaminants: Part A, 27*(1), 36–42. https://doi.org/10.1080/02652030903161598

Campo, M. M., Nute, G. R., Hughes, S. I., Enser, M., Wood, J. D., & Richardson, R. I. (2006). Flavour perception of oxidation in beef. *Meat Science, 72*(2), 303–311. https://doi.org/10.1016/j.meatsci.2005.07.015

Campo, M., Romero, J., Guerrero, A., Resconi, V., Tesniere, G., Santolaria, P., & Olleta, J. (2024). Nutrient composition of beef from the pyrenees. *Journal of Food Composition and Analysis, 133*, Article 106452. https://doi.org/10.1016/j.jfca.2024.106452

Capouya, R., Mitchell, T., Clark, D. I., Clark, D. L., & Bass, P. (2020). A survey of microbial communities on dry-aged beef in commercial meat processing facilities. *Meat and Muscle Biology, 4*(1), 1–11. https://doi.org/10.22175/mmb.10373

Chen, J., Xing, Y., Nie, M., Xu, M., Huang, H., Xie, H., Liao, J., Lin, X., Duan, J., & Zhang, J. (2024). Comparative effects of various dietary selenium sources on growth performance, meat quality, essential trace elements content, and antioxidant

capacity in broilers. *Poultry Science, 103*(9), Article 104057. https://doi.org/10.1016/j.psj.2024.104057
Chong, J., Wishart, D. S., & Xia, J. (2019). Using MetaboAnalyst 4.0 for comprehensive and integrative metabolomics data analysis. *Current Protocols in Bioinformatics, 68*(1), e86. https://doi.org/10.1002/CPBI.86
Dashdorj, D., Tripathi, V. K., Cho, S., Kim, Y., & Hwang, I. (2016). Dry aging of beef; review. *Journal Of Animal Science And Technology, 58*, 20. https://doi.org/10.1186/s40781-016-0101-9
Domínguez, R., Pateiro, M., Gagaoua, M., Barba, F. J., Zhang, W., & Lorenzo, J. M. (2019). A comprehensive review on lipid oxidation in meat and meat products. *Antioxidants, 8*(10), 429. https://doi.org/10.3390/antiox8100429
Dragoev, S. G. (2024). Lipid peroxidation in muscle foods: Impact on quality, safety and human health. *Foods, 13*(5), 797. https://doi.org/10.3390/foods13050797
Faustman, C., Sun, Q., Mancini, R., & Suman, S. P. (2010). Myoglobin and lipid oxidation interactions: Mechanistic bases and control. *Meat Science, 86*(1), 86–94.
Han, J., Wang, Y., Wang, Y., Hao, S., Zhang, K., Tian, J., & Jin, Y. (2024). Effect of changes in the structure of myoglobin on the color of meat products. *Food Materials Research, 4*(e011). https://doi.org/10.48130/fmr-0024-0003
Huff-Lonergan, E., & Lonergan, S. M. (2005). Mechanisms of water-holding capacity of meat: The role of postmortem biochemical and structural changes. *Meat Science, 71*(1), 194–204. https://doi.org/10.1016/J.MEATSCI.2005.04.022
Jung, H. Y., Lee, H. J., Lee, H. J., Kim, Y. Y., & Jo, C. (2024). Exploring effects of organic selenium supplementation on pork loin: Se content, meat quality, antioxidant capacity, and metabolomic profiling during storage. *Journal Of Animal Science And Technology, 66*(3), 587–602. https://doi.org/10.5187/JAST.2023.E62
Juszczak-Czasnojć, M., Tomza-Marciniak, A., Pilarczyk, B., & Gączarzewicz, D. (2023). Total selenium level and its distribution between organs in beef cattle in different selenium status. *Animals, 13*(24), 3885. https://doi.org/10.3390/ani13243885
Khan, M. I., Jung, S., Nam, K. C., & Jo, C. (2016). Postmortem aging of beef with a special reference to the dry aging. *Korean Journal for Food Science of Animal Resources, 36*(2), 159–169. https://doi.org/10.5851/KOSFA.2016.36.2.159
Kim, Y. H. B., Kemp, R., & Samuelsson, L. M. (2016). Effects of dry-aging on meat quality attributes and metabolite profiles of beef loins. *Meat Science, 111*, 168–176. https://doi.org/10.1016/j.meatsci.2015.09.008.
Kim, Y. H. B., Ma, D., Setyabrata, D., Farouk, M. M., Lonergan, S. M., Huff-Lonergan, E., & Hunt, M. C. (2018). Understanding postmortem biochemical processes and post-harvest aging factors to develop novel smart-aging strategies. *Meat Science, 144*, 74–90. https://doi.org/10.1016/j.meatsci.2018.04.031
Koohmaraie, M., & Geesink, G. H. (2006). Contribution of postmortem muscle biochemistry to the delivery of consistent meat quality with particular focus on the calpain system. *Meat Science, 74*(1), 34–43. https://doi.org/10.1016/J.MEATSCI.2006.04.025
Krzywicki, K. (1979). Assessment of relative content of myoglobin, oxymyoglobin and metmyoglobin at the surface of beef. *Meat Science, 3*(1), 1–10. https://doi.org/10.1016/0309-1740(79)90019-6
Litwińczuk, Z., Domaradzki, P., Florek, M., Zółkiewski, P., & Staszowska, A. (2015). Content of macro- and microelements in the meat of young bulls of three native breeds (polish red, white-backed and Polish Black-and-White) in comparison with simmental and Polish holstein-friesian. *Annals of Animal Science, 15*(4), 977–985. https://doi.org/10.1515/aoas-2015-0058
Mancini, R. A., & Hunt, M. C. (2005). Current research in meat color. *Meat Science, 71*(1), 100–121. https://doi.org/10.1016/j.meatsci.2005.03.003
Min, B., & Ahn, D. U. (2005). Mechanism of lipid peroxidation in meat and meat products - A review. *Food Science and Biotechnology, 14*(1), 152–163. https://www.scirp.org/reference/referencespapers?referenceid=2839693.
Mocchegiani, E., Muzzioli, M., & Giacconi, R. (2000). Zinc, metallothioneins, immune responses, survival and ageing. *Biogerontology, 1*(2), 133–143. https://doi.org/10.1023/A:1010095930854
Monteiro, M. L. G., Mutz, Y. S., Francisco, K. A., Rosário, D. K. A., & Conte-Junior, C. A. (2023). Combined UV-C technologies to improve safety and quality of fish and meat products: A systematic review. *Foods, 12*(10), 1961. https://doi.org/10.3390/foods12101961
Patel, N., Bergamaschi, M., Cagnin, M., & Bittante, G. (2020). Exploration of the effect of farm, breed, sex and animal on detailed mineral profile of beef and their latent explanatory factors. *International Journal of Food Science and Technology, 55*(3), 1046–1056. https://doi.org/10.1111/IJFS.14455
Patel, N., Bergamaschi, M., Magro, L., Petrini, A., & Bittante, G. (2019). Relationships of a detailed mineral profile of meat with animal performance and beef quality. *Animals: An Open Access Journal from MDPI, 9*(12), 1073. https://doi.org/10.3390/ani9121073
Pereira, P. M. de C. C., Vicente, A. F., & dos, R. B. (2013). Meat nutritional composition and nutritive role in the human diet. *Meat Science, 93*(3), 586–592. https://doi.org/10.1016/j.meatsci.2012.09.018
Perry, N. (2012). Dry aging beef. *International Journal of Gastronomy and Food Science, 1*(1), 78–80. https://doi.org/10.1016/j.ijgfs.2011.11.005
Pilarczyk, R. (2014). Concentrations of toxic and nutritional essential elements in meat from different beef breeds reared under intensive production systems. *Biological Trace Element Research, 158*(1), 36–44. https://doi.org/10.1007/s12011-014-9913-y
Ramanathan, R., Hunt, M. C., English, A. R., Mafi, G. G., & Vanoverbeke, D. L. (2019). Effects of aging, modified atmospheric packaging, and display time on metmyoglobin reducing activity and oxygen consumption of High-pH beef. *Meat and Muscle Biology, 3*(1), 276–288. https://doi.org/10.22175/mmb2019.05.0017
Ramanathan, R., Hunt, M. C., Mancini, R. A., Nair, M. N., Denzer, M. L., Suman, S. P., & Mafi, G. G. (2020). Recent updates in meat color research: Integrating traditional and high-throughput approaches. *Meat and Muscle Biology, 4*(2), 1–24. https://doi.org/10.22175/mmb.9598
Ramos, A., Cabrera, M. C., & Saadoun, A. (2012). Bioaccessibility of Se, Cu, Zn, Mn and Fe, and heme iron content in unaged and aged meat of Hereford and braford steers fed pasture. *Meat Science, 91*(2), 116–124. https://doi.org/10.1016/j.meatsci.2012.01.001
Ribeiro, F. A., Lau, S. K., Furbeck, R. A., Herrera, N. J., Henriott, M. L., Bland, N. A., Fernando, S. C., Subbiah, J., Sullivan, G. A., & Calkins, C. R. (2021). Ultimate pH effects on dry-aged beef quality. *Meat Science, 172*. https://doi.org/10.1016/j.meatsci.2020.108365
Ribeiro, F. A., Lau, S. K., Pflanzer, S. B., Subbiah, J., & Calkins, C. R. (2021). Color and lipid stability of dry aged beef during retail display. *Meat Science, 171*. https://doi.org/10.1016/j.meatsci.2020.108274
Ribeiro, A., Oliveira, I., Soares, K., Silva, F., Teixeira, P., & Saraiva, C. (2023). Microbial, physicochemical profile and sensory perception of dry-aged beef quality: A preliminary Portuguese contribution to the validation of the dry aging process. *Foods, 12*(24), 4514. https://doi.org/10.3390/foods12244514
Silva, F. L., Oliveira-Júnior, E. S., Silva, M. H. M., López-Alonso, M., & Pierangeli, M. A. P. (2022). Trace elements in beef cattle: A review of the scientific approach from one health perspective. *Animals, 12*(17), 2254. https://doi.org/10.3390/ani12172254
Suman, S. P., & Joseph, P. (2013). Myoglobin chemistry and meat color. *Annual Review of Food Science and Technology, 4*, 79–99. https://doi.org/10.1146/annurev-food-030212-182623
Surai, P. F., Kochish, I. I., Fisinin, V. I., & Juniper, D. T. (2019). Revisiting oxidative stress and the use of organic selenium in dairy cow nutrition. *Animals, 9*, 462. https://doi.org/10.3390/ani9070462
Toldrá, F., & Flores, M. (1998). The role of muscle proteases and lipases in the flavor development of dry-cured ham. *Food Research International, 31*(10), 653–662. https://doi.org/10.1080/10408699891274237
Xue, S., Setyabrata, D., Bonham, C. C., & Kim, Y. H. B. (2021). Evaluation of functional and chemical properties of crust from dry-aged beef loins as a novel food ingredient. *Meat Science, 173*, Article 108403. https://doi.org/10.1016/j.meatsci.2020.108403
Yu, Q., Gu, X., Liu, Q., Wen, R., & Sun, C. (2024). Effect of wet-aging on meat quality and exudate metabolome changes in different beef muscles. *Food Research International, 184*, Article 114260. https://doi.org/10.1016/J.FOODRES.2024.114260
Zhang, S., Xie, Y., Li, M., Yang, H., Li, S., Li, J., Xu, Q., Yang, W., & Jiang, S. (2020). Effects of different selenium sources on meat quality and shelf life of fattening pigs. *Animals, 10*(4), 615. https://doi.org/10.3390/ani10040615